in Table 2 demonstrate, changes in cell density are correlated with changes in ligand clustering and endocytosis. Transglutaminase activity in cells varies with cell density[24], with changes in intracellular cyclic AMP[25] and in response to viral transformation[24]. Such alterations in transglutaminase activity may be reflected in an alteration in the ability of cells to internalise surface-bound ligands. Maxfield *et al.*[31] have shown that blocking EGF internalisation with inhibitors of transglutaminase produced marked stimulation in the mitogenic response of cells to the hormone. Changes in transglutaminase activity may therefore profoundly modify the way that cells respond to hormones.

We thank Dr Jack Folk, NIH for the gift of various peptide inhibitors of transglutaminase and for stimulating discussions, Maria Gallo for preparing $\alpha_2$-macroglobulin, and Elizabeth Lovelace for help with cultured cells. A.L. is on leave of absence from the Department of Biological Chemistry, the Hebrew University of Jerusalem, Israel.

Received 26 June; accepted 2 November 1979.

1. Anderson, R. G. W., Brown, M. S. & Goldstein, J. L. *Cell* **10**, 351–364 (1977).
2. Maxfield, F. R., Schlessinger, J., Schechter, Y., Pastan, I. & Willingham, M. C. *Cell* **14**, 805–810 (1978).
3. Maxfield, F. R., Willingham, M. C., Schlessinger, J., Davies, P. J. A. & Pastan, I. *Cold Spring. Harb. Conf. Cell Proliferation* **6**, 159–166 (1979).
4. Willingham, M. C., Maxfield, F. R. & Pastan, I. *J. Cell Biol.* **82**, 614–625 (1979).
5. Van Leuven, F., Cassiman, J. J. & Vandenberghe, H. *J. biol. Chem.* **254**, 5155–5160 (1979).
6. Neufeld, E. F., Sando, G. N., Garvin, A. J. & Rome, L. H. *J. supramolec. Struct.* **6**, 95–101 (1977).
7. Kaplan, A., Achord, D. T. & Sly, W. S. *Proc. natn. Acad. Sci. U.S.A.* **74**, 2026–2030 (1977).
8. Schlessinger, J., Schechter, Y., Willingham, M. C. & Pastan, I. *Proc. natn. Acad. Sci. U.S.A.* **75**, 2659–2663 (1978).
9. Schlessinger, J., Schechter, Y., Cuatrecasas, P., Willingham, M. C. & Pastan, I. *Proc. natn. Acad. Sci. U.S.A.* **75**, 5353–5357 (1978).
10. Haigler, H., Ash, J. F., Singer, S. J. & Cohen, S. *Proc. natn. Acad. Sci. U.S.A.* **75**, 3317–3321 (1978).
11. Haigler, H. T., McKanna, J. A. & Cohen, S. *J. Cell Biol.* **81**, 382–395 (1979).
12. Gorden, P., Cartentier, J., Cohen, S. & Orci, L. *Proc. natn. Acad. Sci. U.S.A.* **75**, 5025–5029 (1978).
13. Maxfield, F. R., Willingham, M. C., Davies, P. J. A. & Pastan, I. *Nature* **277**, 661–663 (1979).
14. Folk, J. E. & Finlayson, J. S. *Adv. Protein Chem.* **31**, 1–133 (1977).
15. Schrode, J. & Folk, J. E. *J. biol. Chem.* **254**, 653–661 (1979).
16. Lorand, L. *et al. Biochemistry* **18**, 1756–1765 (1979).
17. Clarke, D. D., Neidle, A., Sarkar, N. K. & Waelsch, H. *Archs Biochem. Biophys.* **79**, 338–354 (1959).
18. Lorand, L., Campbell-Wilkes, L. K. & Cooperstein, L. *Analyt. Biochem.* **50**, 623–631 (1972).
19. Nillson, J. L. G. *et al. Ann. N. Y. Acad. Sci.* **202**, 286–296 (1972).
20. Desbuquois, B., Krug, F. & Cuatrecasas, P. *Biochim. biophys. Acta* **343**, 101–120 (1974).
21. Willingham, M. C., Yamada, S. S. & Pastan, I. *Proc. natn. Acad. Sci. U.S.A.* **75**, 4359–4363 (1978).
22. Willingham, M. C. & Pastan, I. *Cell* **13**, 501–507 (1978).
23. Pohjanpelto, P. *J. Cell Biol.* **68**, 512–520 (1976).
24. Birckbichler, P. J., Orr, G. R., Conway, E. & Patterson, N. K. *Cancer Res.* **37**, 1340–1344 (1977).
25. Milhaud, P., Davies, P. J. A., Gottesman, M. & Pastan, I. *Biochim. biophys. Acta* (submitted).
26. Davies, P. J. A., Davies, D. R., Maxfield, F. R., Willingham, M. C. & Pastan, I. (in preparation).
27. Fesus, L. & Laki, K. *Biochemistry* **16**, 4061–4066 (1977).
28. Novogrodsky, A., Quittner, S., Rubin, A. L. & Stengel, K. H. *Proc. natn. Acad. Sci. U.S.A.* **75**, 1157–1161 (1978).
29. Baker, J. B., Simmer, R. L., Glenn, K. C. & Cunningham, D. D. *Nature* **278**, 743–745 (1979).
30. Linsley, P. S., Blifeld, C., Wrann, M. & Fox, C. F. *Nature* **278**, 745–748 (1979).
31. Maxfield, F. R., Davies, P. J. A., Klempner, L., Willingham, M. C. & Pastan, I. *Proc. natn. Acad. Sci. U.S.A.* **76**, 5731–5735 (1979).

# Mapping of metabolites in whole animals by $^{31}$P NMR using surface coils

**Joseph J. H. Ackerman, Thomas H. Grove, Gordon G. Wong, David G. Gadian & George K. Radda**

Department of Biochemistry, Oxford University, South Parks Road, Oxford, UK

*The metabolic state of skeletal muscle and brain within intact rats is monitored using high resolution phosphorus nuclear magnetic resonance. Regional disturbances in metabolism (for example, localised ischaemia) are easily observed, indicating the diagnostic possibilities of the method. Measurements are made using 'surface' radiofrequency coils, which we discuss in detail.*

IT was demonstrated in 1974 that phosphorus nuclear magnetic resonance ($^{31}$P NMR) can be used to observe the major phosphorus-containing metabolites in intact, excised muscle[1]. Since then the method, which is non-destructive, has been used to study a variety of biochemical, physiological and medical problems in skeletal muscle[2,3], heart[4,5], kidney[6], liver[7] and brain[8] (for reviews see refs 9–11). Apart from the measurements on mouse brain[8] and the recent experiments on heart in open-chested rats[12,13], all these studies were done on excised organs, albeit often in a physiologically functional state.

Recently, 'spin-imaging' of water in living systems has demonstrated the ability of NMR to obtain spatial discrimination[14]. The combination of high resolution $^{31}$P NMR with some method of spatial selection could offer a unique opportunity for the study of metabolism in defined tissues and organs of an intact animal. However, because of the low sensitivity and difficulties with spectral resolution, many of the methods used in water imaging are not yet practical for $^{31}$P spin-imaging of living systems. We describe here a simple method for detecting compounds in localised regions adjacent to the surface of the sample. We have used an unusual type of radiofrequency coil, which we call 'surface coil', to obtain the NMR signal. In this article we discuss the theory of the method, describe experiments on test phantoms, and show the application of the technique to the study of muscle and brain metabolism in living animals.

## Theory and design of surface coils

The design of radiofrequency (r.f.) coils is best considered in terms of the theory of Hoult and Richards[15]. Let us consider a single r.f. coil that serves the role of both transmitter and receiver. Their theory shows that:

(1) The signal-to-noise ratio resulting from a 90° r.f. pulse applied to a small sample at point $q$ is proportional to the value of $(B_1)_{xy}$ at that point. $(B_1)_{xy}$ is the component of the r.f. magnetic field in the $xy$ plane (that is, in the plane perpendicular to the static field $B_0$) that is generated by unit current passing through the coil.
(2) The 90° pulse length for a sample at any point $q$ is inversely proportional to the value of $(B_1)_{xy}$ at that point.
(3) The signal-to-noise ratio resulting from a single r.f. pulse of angle $\phi$ is proportional to $(B_1)_{xy} \sin\phi$. $\phi$ is equal to $\gamma(B_1)_{xy} i\tau$ where $\tau$ is the length of the pulse, $\gamma$ is the magnetogyric ratio of the nucleus, and $i$ is the current passing through the coil.

0028-0836/80/020167—04$01.00

Clearly the field distribution $(B_1)_{xy}$ produced by the coil is a critical factor in its performance. Conventional saddle-shaped and solenoidal coils are generally designed to produce a homogeneous $B_1$ field throughout the sample volume; this ensures that all regions of a uniform sample contribute equally to the signal. In contrast, we show that a different coil design enables us to observe signals from a selected region adjacent to the surface of the sample.

Consider a single-turn flat circular coil orientated as in Fig. 1. The magnetic field generated at any point $q$ by unit current flowing in the coil is given by Smythe[16] and is

$$B_\rho = \frac{\mu}{2\pi}\frac{x}{\rho[(a+\rho)^2+x^2]^{1/2}}\left[-K+\frac{a^2+\rho^2+x^2}{(a-\rho)^2+x^2}E\right] \quad (1)$$

$$B_x = \frac{\mu}{2\pi}\frac{1}{[(a+\rho)^2+x^2]^{1/2}}\left[K+\frac{a^2-\rho^2-x^2}{(a-\rho)^2+x^2}E\right] \quad (2)$$

$B_x$ and $B_\rho$ are the axial ($x$) and radial ($\rho$) components of the field at point $q$, $a$ is the coil radius, $\mu$ the permeability of the medium about the coil and $K$ and $E$ are complete elliptic integrals of the first and second kind.

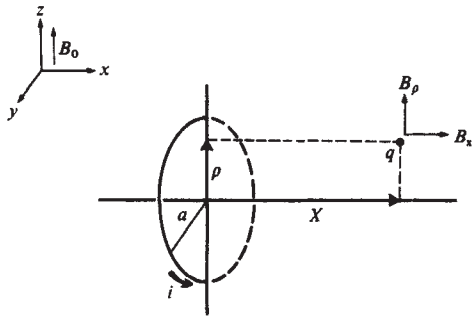


**Fig. 1** Diagram illustrating the orientation of a single loop coil. Various parameters are $B_0$, the main magnetic field, $a$, the coil radius, $i$, the current flowing in the coil, and $q$, a point in space described by the coordinates ($\rho$, $x$). $B_\rho$ and $B_x$ are the $B_1$ field components at $q$ resulting from current $i$. The angle $\theta$ formed by the vector $\rho$ and $B_0$ is shown as 0 for clarity of presentation.

From Fig. 1, we see that the direction of $B_x$ is always perpendicular to that of the static field $B_0$, while the perpendicular component of $B_\rho[(B_\rho)_{xy}]$ is given by

$$(B_\rho)_{xy} = B_\rho \sin\theta \quad (3)$$

where $\theta$ is the angle between the directions of $B_\rho$ and $B_0$ (see Fig. 1 where $\theta = 0$ for clarity of presentation). The magnetic field $(B_1)_{xy}$ generated at any point $q$ therefore depends on $\theta$ and is given by

$$\overline{(B_1)}_{xy} = \overline{B}_x + \overline{(B_\rho)}_{xy} \quad (4)$$

A plot of $(B_1)_{xy}$ as a function of $\rho$ derived from equations (1)–(4) is given in Fig. 2 for the two extremes $\theta = 0$ and $\theta = \pi/2$.

Following from the relationships given above (points (1) to (3)), it is possible to map the $(B_1)_{xy}$ field of any r.f. coil. We have mapped $(B_1)_{xy}$ for a single-turn flat circular coil of radius 0.75 cm by placing a small sample (a disk of volume 0.01 ml containing 12 M phosphoric acid and 4 mM $NiCl_2$) at different positions $q$ relative to the coil. The field $(B_1)_{xy}$ as determined from the variation in signal intensity is plotted in Fig. 2 and, as can be seen, shows good agreement with theory. Similar agreement was obtained from the variation in 90° pulse length, and from experiments with other surface coils. Note that the $^{31}P$ test sample was surrounded by an aqueous medium of 154 mM NaCl to approximate the electrical characteristics of animal tissue.

$(B_1)_{xy}$ is localised in a volume about the centre of the coil roughly defined by the coil radius (Fig. 2). It should therefore be possible to observe high resolution NMR signals from selected regions adjacent to the surface of the samples. Furthermore, we should stress that the region of sample contributing significant signal intensity will be spatially far more sharply defined than $(B_1)_{xy}$ due to the sine term in point (3) above.

Finally, as Hoult and Richards[15] have suggested, variations in phase of $(B_1)_{xy}$ should not affect this type of single coil experiment. This is because phase changes induced at transmission are mirrored at reception, and thus cancel. This conclusion was confirmed by our experiments.

## Experiments with phantoms

To verify and more clearly illustrate the spatial resolution of surface coils, $^{31}P$ NMR experiments were performed on two different phantom samples. The first sample consisted of a two compartment rectangular box (10×2×1 cm) partitioned by a thin panel halfway along the length (5 cm) and filled with a solution of $Na_2HPO_4$ (100 mM) in one compartment and phosphocreatine (100 mM) in the other. $^{31}P$ NMR spectra were collected using a flat four-turn surface coil (mean radius 0.55 cm) placed outside the box at various positions along its length. The results are shown in Fig. 3. With the coil placed directly over the dividing partition, position 0.0, both compartments contribute equal signal intensity. When the centre of the coil is one radius from either side of the partition, only that compartment directly beneath the coil gives a signal. Thus sample selectivity (as a function of the radial, $\rho$, coordinate) is approximately confined to an area bounded by the coil circumference.

The second phantom consisted of a box (4×3×3 cm) filled with an aqueous solution of $NaH_2PO_4$ (20 mM) and NaCl (100 mM). The same coil was placed on the outside of the box (wall thickness 0.1 cm) and the $^{31}P$ spectrum obtained. A hollow

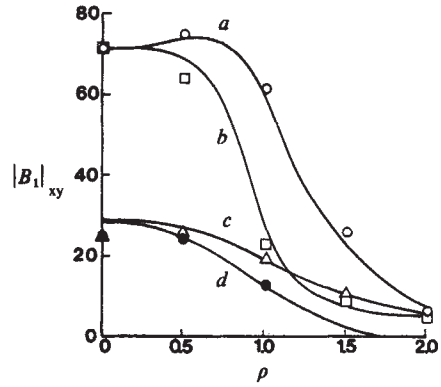


**Fig. 2** The spatial dependence of $(B_1)_{xy}$ as a function of $\rho$, the radial coordinate. $\rho$ is expressed in units of radius, $a$, while $(B_1)_{xy}$ is normalised to 100 at the centre of the coil, $(\rho, x) = (0, 0)$. The solid curves were derived from equations (1)–(4) while the symbols represent experimental data. Spatial parameters vary for each curve as follows: curve $a$, $\theta = \pi/2$ and $x \simeq 0.5a$; curve $b$, $\theta = 0$ and $x \simeq 0.5a$; curve $c$, $\theta = \pi/2$ and $x \simeq 1.1a$; curve $d$, $\theta = 0$ and $x \simeq 1.1a$.

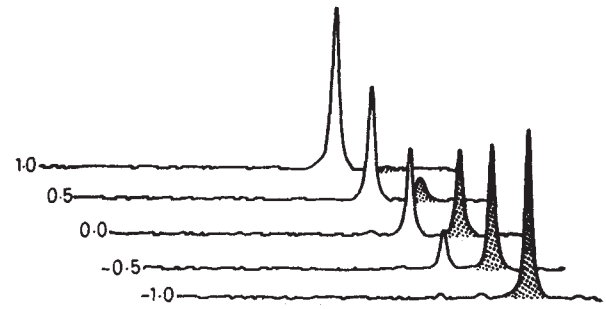


**Fig. 3** Stacked plot demonstrating the radial, $\rho$, resolution of surface coils. The two $^{31}P$ resonances, each arising from a separate compartment in the phantom, are phosphocreatine (shaded) and inorganic phosphate ($Na_2HPO_4$) (non-shaded). The label associated with each spectrum is the distance (in units of coil radius, $a$) between the surface coil centre and the partition which separates the two compartments.

glass disk of radius 0.75 cm and thickness 0.5 cm filled with a solution of NaCl (154 mM) was then placed in the solution-filled box, immediately in front of the coil. On repeating the measurement, a sixfold reduction in signal intensity was observed. This results from the exclusion of 0.8 ml of the $NaH_2PO_4$ solution in front of the coil, illustrating the three-dimensional spatial selectivity of this type of NMR coil.

These experiments verify the theoretical predictions (Fig. 2) and the properties of these coils can be summarised as follows: (1) The high resolution NMR experiment can be performed with a surface coil external to the sample; (2) the spatial resolution is well defined and can be theoretically and experimentally determined; (3) this spatial resolution may be adjusted by appropriate choice of coil radius and pulse width; (4) the filling factors of surface coils compare favourably with those of conventional coils; and (5) noise generated by r.f. losses in conducting samples[17] arise only from those regions of the samples that contribute signal. These latter two points suggest that good signal-to-noise ratios can be expected with well-designed surface coils.

## Measurements of metabolites in whole animals

The results and calculations presented above, together with studies on tissues and perfused organs provided the rationale for attempting to observe $^{31}P$ NMR spectra from muscle and brain of an intact rat.

Figure 4*a* shows the $^{31}P$ NMR spectrum obtained by placing the four-turn surface coil against the leg of an anaesthetised rat. The resonances arise from the three phosphates of ATP, phosphocreatine and inorganic phosphate ($P_i$), within the leg muscle. $^{31}P$ signals contributed by blood within the muscle tissue are negligible as fresh blood contains only a small amount of ATP and no phosphocreatine relative to 2,3-diphosphoglycerate[18]. (If 2,3-diphosphoglycerate were present in significant quantities, it would produce two signals with chemical shifts of about 5 and 6.5 p.p.m.)

To achieve conditions where peak areas are directly proportional to the amounts of tissue metabolites, a 12-s delay was used between sampling pulses. (This follows from the $^{31}P$ $T_1$ relaxation times for intracellular $\beta$-ATP (~1 s), phosphocreatine (~3 s) and inorganic phosphate (~3 s).) Thus the spectral accumulation of 128 scans required about 25 min. However, by reducing the delay between pulses, satisfactory spectra can be recorded in less than a minute. These can be used to follow changes in metabolites, to compare different metabolic states, or even to perform quantitative studies if the appropriate relaxation times or saturation factors are accurately determined[10].

A measure of the ATP concentration is obtained from the area of the signal at −16 p.p.m. (the $\beta$-phosphate peak of ATP). The resonance at −2.4 p.p.m. contains contributions from the $\gamma$-phosphate of ATP and the $\beta$-phosphate of mobile ADP. As the ratio of the areas of these two peaks ([ATP]/[ADP]+[ATP]) is one, within experimental error (0.94, $n = 5$, s.e.m. ± 0.05) clearly the concentration of mobile ADP is too low to be observed. The phosphocreatine to ATP ratio is 4.04 ± 0.18 ($n = 5$) which compares reasonably with recent freeze clamping values for rat skeletal muscle[19] but is considerably higher than other reported values[20]. Because phosphocreatine is rapidly degraded during ischaemia[1] we suggest that our *in vivo* ratio of phosphocreatine to ATP represents the best estimate so far for this parameter that reflects the energy status of the cell. The measurement of inorganic phosphate by freeze extraction procedures provides special difficulties, and it is significant that the NMR results give a phosphocreatine: $P_i$ ratio of 14.6 ($n = 5$; s.e.m. ± 1.20). Assuming a phosphocreatine concentration of 23.1 μmol per g wet wt (ref. 19), the $P_i$ concentration derived from NMR is 1.6 μmol per g wet wt, a value considerably lower than that derived from freeze clamping techniques[20]. This observation might explain why the activity of phosphorylase *b* in resting muscle is considerably less than that predicted by studies on the isolated enzyme combined with metabolic measurements by freeze extraction[21].

Following the observations of Moon and Richards[22] it has been well established that the position of the inorganic phosphate resonance provides a good measure of intracellular *p*H

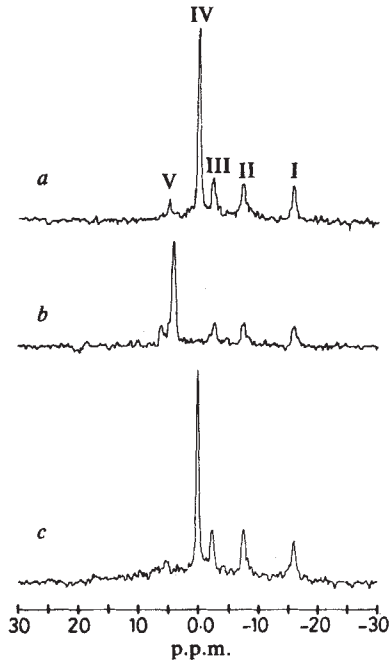


**Fig. 4** $^{31}P$ NMR spectra of the leg muscle of an intact rat obtained with a surface coil. Each spectrum represents 128 scans over 25 min. A 15-Hz line-broadening exponential multiplication was used to enhance signal-to-noise. *a*, Non-ischaemic muscle below the knee joint; *b*, ischaemic muscle from the same area as in *a* after application of a tourniquet just above the knee; *c*, spectrum of muscle above the tourniquet. Chemical shift assignments for non-ischaemic rat leg muscle are $\beta$-phosphate of ATP (I), −16.10 ($n = 5$, s.e.m. ± 0.02), $\alpha$-phosphate (II), −7.54 ($n = 5$, ±0.00), $\gamma$-phosphate of ATP (III), −2.47 ($n = 5$, ±0.02), phosphocreatine (IV), 0.00 by definition, and inorganic phosphate (V), 4.90 ($n = 5$, ±0.03). Chemical shifts are defined as positive in the high frequency direction and phosphocreatine is taken as an internal reference. Normally fed, pentabarbital anaesthetised male Wistar rats were used for all experiments. The rats were examined while in a vertical position. All experiments were done at 73.8 MHz on a spectrometer equipped with a wide-bore magnet.

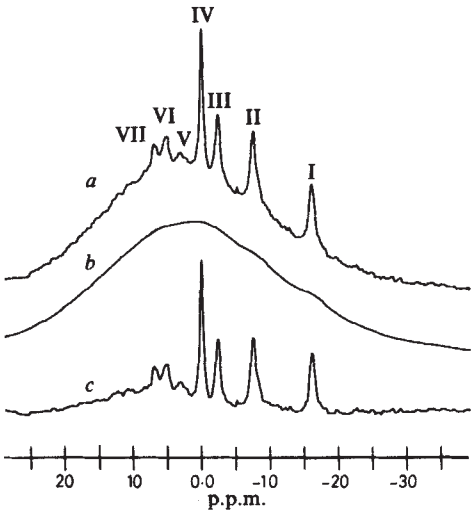


**Fig. 5** $^{31}$P NMR spectra of the brain of an intact rat obtained with a surface coil. Spectra *a–c* demonstrate the effects of the convolution difference technique in eliminating the broad $^{31}$P component arising from bone. *a*, Original brain spectrum, 300 data accumulations over 60 min with a 15-Hz line broadening exponential multiplication; *b*, same as *a* except a 400-Hz line broadening exponential multiplication was used; *c*, difference spectrum of *a* minus *b*. Chemical shift assignments are $\beta$-phosphate of ATP (I), −16.20 ($n = 5$, ±0.05), $\alpha$-phosphate of ATP (II), −7.62 ($n = 5$, ±0.02), $\gamma$-phosphate of ATP (III), −2.48 ($n = 5$, ±0.02), phosphocreatine (IV) 0.00 by definition, phosphodiesters (V) 3.0 ($n = 3$, ±0.1), inorganic phosphate and the 2-phosphate of 2,3-diphosphoglycerate (VI), 5.00 ($n = 5$, ±0.007), and sugar phosphates and the 3-phosphate of 2,3-diphosphoglycerate (VII), 6.65 ($n = 5$, ±0.06).

(refs 9, 10). The chemical shift of $P_i$ within rat leg muscle is $4.90 \pm 0.03$ ($n = 5$), consistent with a *p*H of $7.1 \pm 0.02$ ($n = 5$).

In an experiment similar in philosophy to the two compartment phantom, the effect of localised ischaemia in the rat leg muscle was assessed (Fig. 4). A control muscle spectrum was obtained from just below the knee joint (Fig. 4*a*). Then a very tight tourniquet was placed around the leg just above the knee and a spectrum obtained from the same location as the initial control (Fig. 4*b*). The two spectra are significantly different. The ischaemic region of the muscle has no phosphocreatine, somewhat reduced amounts of ATP and a very large $P_i$ concentration. In addition, the $P_i$ chemical shift (4.31 p.p.m.) differs significantly from that in the control muscle (4.92 p.p.m.), indicating a more acidic *p*H of 6.7. (Similar results with excised tissue have been observed[1–3].) The small new peak at 6.30 p.p.m. may be attributable to the build-up of sugar phosphates or nucleotide monophosphate. Finally, with the tourniquet still in place, a spectrum was obtained from the leg muscle above the tourniquet (Fig. 4*c*). This spectrum is very similar to that of the first control, indicating healthy, non-ischaemic muscle. The localisation of ischaemic areas in diseased muscle is thus clearly possible.

One of the most difficult organs to study by biochemical and perfusion techniques is the brain. Because of the rapid oxidative metabolism and sensitivity to short periods of hypoxia or ischaemia of the brain, considerable effort has been spent in developing a variety of techniques such as 'freeze-blowing'[23], and cryo-NMR[8] to assess the *in vivo* energy status of this tissue.

By placing a surface coil on top of the rat's head, directly over the brain, we were able to obtain excellent $^{31}$P spectra from the brain (Fig. 5). As there is no muscle tissue between the coil and the brain these experiments are selective for brain tissue and bone only. The very broad contribution from the bone can easily be eliminated by the convolution difference technique[24].

From the chemical shifts of the three ATP resonances in brain and muscle we can conclude that in both tissues the ATP is predominantly complexed to divalent cations which we assume to be $Mg^{2+}$.

The energy status of the live brain may be best compared with that of perfused or rapidly frozen tissue from the value of the phosphocreatine to ATP ratio. The value we derived from NMR ($1.93 \pm 0.12$, $n = 5$) is higher than the best values obtained by rapid freezing[23]. In addition we estimate that the concentrations of both mobile ADP and $P_i$ are much lower than those measured by destructive analytical techniques. In the brain spectrum the ratio of the resonances $\beta$-phosphate of ATP: $\gamma$-phosphate of ATP + $\beta$-phosphate of ADP is $1.07 \pm 0.08$ ($n = 5$) indicating that ADP is not detectable. The $P_i$ signal is obscured by the 2-phosphate peak of 2,3-diphosphoglycerate present in blood. The 3-phosphate from the same compound is at 6.6 p.p.m. and indicates that the $P_i$ concentration in the brain must be well below that of ATP, in contrast to values obtained from freeze extraction. These considerations lead to the conclusion that the phosphorylation state in brain tissue ($[ATP]/[ADP][HPO_4^{2-}]$) is at least an order of magnitude higher than the generally accepted value of $\sim 3{,}400\ M^{-1}$.

## Conclusions

The use of surface coils to obtain high resolution NMR spectra from selected regions of large objects is clearly not limited to the systems described here. The design of the coil can be adapted to suit the sample. In animals, tissues other than muscle and brain (for example, fat tissue or cancerous growth) could be studied. Coupled with surgery, internal organs can easily be investigated[12].

An early low resolution application of flat coils has been for the measurement of blood flow[25]. Plant, fungal or non-living materials can also be examined in this way.

This work was supported by the SRC, NIH and the British Heart Foundation. T.H.G. is a NATO Fellow in Science, J.J.H.A. a NIH postdoctoral fellow and G.G.W. is a Rhodes Scholar. We thank Mr P. Styles for his help and Sir Rex Richards for his support.

Received 9 October; accepted 12 November 1979.

1. Hoult, D. I. *et al. Nature* **252,** 285–287 (1974).
2. Dawson, M. J., Gadian, D. G. & Wilkie, D. R. *Nature* **274,** 861–866 (1978).
3. Burt, C. T., Glonek, T. & Barany, M. *J. biol. Chem.* **251,** 2584–2591 (1976).
4. Jacobus, W. E., Taylor IV, G. J., Hollis, D. P. & Nunnally, R. L. *Nature* **265,** 756–758 (1977).
5. Garlick, P. B., Radda, G. K., Seeley, P. J. & Chance, B. *Biochem. biophys. Res. Commun.* **74,** 1256–1262 (1977).
6. Sehr, P. A., Radda, G. K., Bore, P. J. & Sells, R. A. *Biochem. biophys. Res. Commun.* **77,** 195–202 (1977).
7. Salhany, J. M., Stohs, S. J., Reinke, L. A., Pieper, G. M. & Hassing, J. M. *Biochem. biophys. Res. Commun.* **86,** 1077–1083 (1979).
8. Chance, B., Nakase, Y., Bond, M., Leigh, J. S. & McDonald, G. *Proc. natn. Acad. Sci. U.S.A.* **75,** 4925–4929 (1978).
9. Radda, G. K. & Seeley, P. J. *A. Rev. Physiol.* **41,** 749–769 (1979).
10. Gadian, D. G., Radda, G. K., Richards, R. E. & Seeley, P. J. in *Biological Applications of Magnetic Resonance* (ed. Shulman, R. G.) 463–535 (Academic, New York, 1979).
11. Burt, C. T., Cohen, S. M. & Barany, M. *A. Rev. Biophys. Bioengng* **8,** 1–25 (1979).
12. Ackerman, J. J. H., Bore, P. J., Gadian, D. G., Grove, T. H. & Radda, G. K. *Phil. Trans. R. Soc.* (in the press).
13. Grove, T. H., Ackerman, J. J. H., Radda, G. K. & Bore, P. J. *Proc. natn. Acad. Sci. U.S.A.* (in the press).
14. Williams, R. J. P., Andrew, E. R. & Radda, G. K. (eds) *NMR of Intact Biological Systems Phil. Trans. R. Soc.* (in the press).
15. Hoult, D. I. & Richards, R. E. *J. Magn. Resonance* **24,** 71–85 (1976).
16. Smythe, W. R. *Static and Dynamic Electricity* 3rd edn, 291 (McGraw-Hill, New York, 1968).
17. Hoult, D. I. & Lauterbur, P. C. *J. Magn. Resonance* **34,** 425–433 (1979).
18. Henderson, J. O., Costello, A. J. R. & Omachi, A. *Proc. natn. Acad. Sci. U.S.A.* **71,** 2487–2490 (1974).
19. Beis, I. & Newsholme, E. A. *Biochem. J.* **152,** 23–32 (1975).
20. Williamson, D. H. & Brosnan, J. T. in *Methods of Enzymatic Analysis* Vol. 4 (ed. Bergmeyer, H. U.) 2266–2302 (Academic, New York, 1974).
21. Busby, S. J. W. & Radda, G. K. *Curr. Topics cell. Regulation* **10,** 89–160 (1976).
22. Moon, R. B. & Richards, J. H. *J. biol. Chem.* **248,** 7276–7278 (1973).
23. Veech, R. L., Harris, R. L., Veloso, D. & Veech, E. H. *J. Neurochem.* **20,** 183–188 (1973).
24. Campbell, I. D., Dobson, C. M., Williams, R. J. P. & Xavier, A. V. *J. Magn. Resonance* **11,** 172–181 (1973).
25. Morse, O. C. & Singer, J. R. *Science* **170,** 440–441 (1970).